

Optimal Design of Medium Voltage Composite Insulator Profiles Using Finite Element Method and Artificial Neural Networks

Elhadj HABEL^{1*}, Mohamed MARICH¹

¹Departement of Science and Technology, Faculty of Science and Technology, University Ahmed Benyahia El-Wancharissi of Tissemsilt, Bougara Ben Hamouda road, 38000 Tissemsilt, Algeria;

*Corresponding author: Elhadj HABEL, Email: habel.hadj@univ-tissemsilt.dz

ARTICLE INFO

Received: 25 Dec 2024
Revised: 20 Apr 2025
Accepted: 08 Nov 2025

ABSTRACT

Polymeric insulators are extensively used in high-voltage applications due to their performance hydrophobic properties. Electrical field distribution along the insulator surface is considered one of the important parameters for the performance evaluation of outdoor insulators. Reliability of medium voltage composite insulators depends on achieving an optimal electrical and geometrical design that produces the lowest electric field strength. This paper proposes a method to find the optimal geometrical design of composite insulators for different voltage levels. This method combined Finite Element Method (FEM) and Artificial Neural Networks (ANN). First, it was used the FEM to evaluate the influence of insulator geometrical parameters on the electric field strength such as shed radius, core diameter, shed inclination angle and distance between the first shed and end fitting. The electric field strength was calculated by using the commercial software package COMSOL Multiphysics. Then, the ANN algorithm has been implemented using the MATLAB program to improve the electric field distribution of composite insulators by reducing the value of maximum electric field strength in order to optimize the original profile that produces the lowest electric field strength. The results of this study are able to provide theoretical support to design and select the suitable profile of composite insulators in order to obtain better performance.

Keywords: Composite insulators, Electric field, Artificial Neural Networks (ANN), Finite Element Method (FEM).

INTRODUCTION

Polymeric insulators are mainly used for outdoor applications as replacement for conventional glass and porcelain insulation systems. They have started to gain popularity amongst electric power utilities due to their lightweight and outstanding electrical performance in moderate to heavily polluted environments [1-3]. The reliability of the power grid is directly correlated with its performance. Therefore, the power grid operation and maintenance department pays close attention to the composite insulators [4-6]. The study of electric field distribution along polymeric insulators is very important for understanding the discharge mechanism and pollution flashover. Moreover, the electric field study gives an indication of the possible damage and service life of the insulator under contamination [7-9]. Electrical design now heavily relies on numerical techniques as reliable and precise methods for electric field computation [10]. Numerical analysis techniques are used to investigate the electric field distribution of polymeric insulators [3,11]. With readily available computational power, issues related to the electric field, governed by Maxwell's equations, are commonly addressed using the robust FEM [3,12].

In the last years, the computational intelligence techniques have been successfully applied in many studies. Among these methods, artificial neural network (ANN) architectures have been widely used, due to their computational speed, the ability to handle complex non-linear functions, robustness and great efficiency, even in cases where full information for the studied problem is absent. The ANNs, present to have applications in the solution of various engineering problems, such as function approximation, modeling, classification, control, estimation and prediction, etc. In the field of high voltage (HV), ANNs have been used to estimate the time-to-flashover [13,14], to analyze the insulator surface tracking on solid insulators [15], to estimate the pollution level [16], and to predict a flashover

voltage [17,18].

This paper proposes an ANN model coupled with finite-element method (FEM), which will be used to estimate the maximal electric field on medium voltage insulator surfaces to find the optimal geometrical design of 11 kV composite insulators that produce the lowest electric field strength for different voltage levels.

ELECTRIC FIELD CALCULATION USING FEM

Finite element method is used in this paper, and has been widely used in electrical engineering as a main numerical calculation method for quantifiably analyzing the performance of insulators under electromagnetic fields. The finite element method for any problem consists of, basically, discretizing the solution domain to a finite number of elements, deriving governing equations for a typical element, assembling all elements in the solution domain, and solving the system of equations. As a consequence, the electrostatic field finite element method is used to calculate the electric field distribution along the insulator. Simply, the way for electric field distribution calculation is to calculate electric potential distribution. Then, electric field distribution is calculated by the minus gradient of electric potential distribution. Due to electrostatic field distribution, electric field distribution can be written as follows:

$$E = -\nabla.V \quad (1)$$

From Maxwell's equation:

$$\nabla.E = \frac{\rho}{\epsilon_0\epsilon_r} \quad (2)$$

Where ρ is Volume Charge Density in C/m³, ϵ_0 is air dielectric constant which equals 8.85×10^{-12} F/m and ϵ_r is relative dielectric constant of dielectric material, then place equation (1) in equation (2), obtain Poisson's equation.

$$\Delta V = -\frac{\rho}{\epsilon} \quad (3)$$

Without space charge $\rho = 0$, Poisson's equation becomes Laplace's equation:

$$\Delta V = 0 \quad (4)$$

In this model, as the insulator structure is cylindrical in shape, the modeling can be simplified into a two-dimension (2D) model in preference to a full three-dimension (3D) model that uses much computer memory. This simplification saves the considerable size of memory and processing time without affecting the accuracy of the simulation results.

1. Simulation of the typical composite insulator used:

A non-ceramic insulator has four main components. They are the fiberglass rod, polymer sheath on the rod, polymer weather sheds, and two metal end fittings. The insulator investigated in this study is a standard 11 kV polymeric insulator. The structure of this model is shown in Figure 1.

Dimensions and material properties of the 11 kV silicone rubber insulators used in the simulation study are shown in Tables 1 and 2.

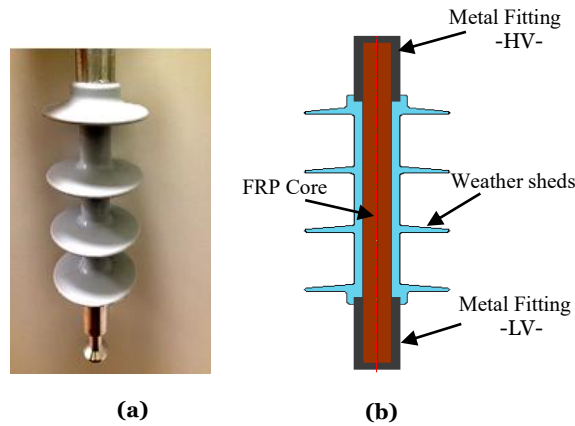


Figure 1: An 11 kV silicone rubber insulator: (a) insulator geometry, (b) cross-sectional profile.

Table 1: Insulator parameter.

Dimension	mm
Creepage distance	375
Shed diameter	90
Shed separation	46
Height (End fitting separation)	175
Trunk diameter	28
Inner core diameter	18

Table 2: Material properties for the used insulator.

Materials	Relative Permittivity ϵ_r	Conductivity σ ($\mu\text{S/cm}$)
Air	1.0	1.0×10^{-15}
SIR	4.3	1.0×10^{-13}
FRP core	7.1	1.0×10^{-13}
Metal Fitting	1.0	6.0×10^6
Water droplet	80	5.5×10^{-6}

2. Analysis of design parameters:

In order to study the effects of the various geometrical parameters on the design of the clean silicone rubber insulator. Effect of variation of shed radius, shed’s inclination angle radius, diameter of core, and distance from the shed to the end fitting on the electric field distribution has been studied. One parameter is varied keeping the other three parameters constant as per manufacturer. The electrostatic formulation of AC/DC physics was used for all simulations.

2.1. Effect of the distance between the first shed and end fitting:

The fitting distance from the first shed to the end fitting of the insulator was varied to simulate and study its effect on electric field distribution along the silicon insulator (Figure 2).

From Figure 3, it is comprehended that the highest distance between the first shed and the bottom end fitting generally yields a lower electric field stress, while the shortest distance gives the highest increment in electric field stress. Hence, it can be concluded from Figure 3 that as the distance between the first shed and the bottom end fitting increases, the electric field stress at the first shed decreases [19].

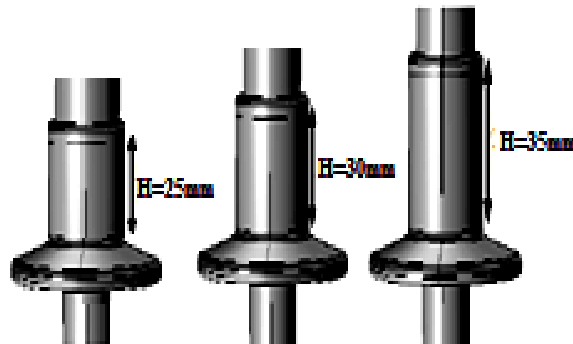


Figure 2: Change of fitting distance.

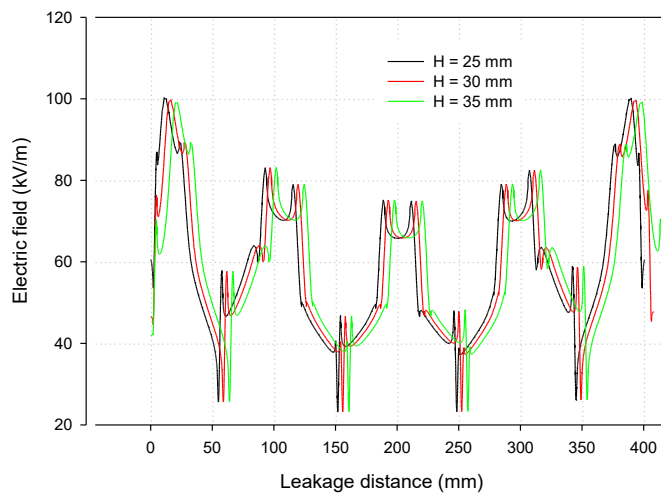


Figure 3: Electric field with different distance between the first shed and end fitting.

2.2. Effect of the core's diameter:

In this case, the Core's Diameter of the insulator was varied to simulate and study its effect on electric field distribution along the silicon insulator (Figure 4).

The electric field near the electrodes increases with increasing core diameter, while in the middle of the insulator. The electric field tends to decrease with increasing diameter of the core insulator as shown in Figure 5.



Figure 4: Change of Core's Diameter.

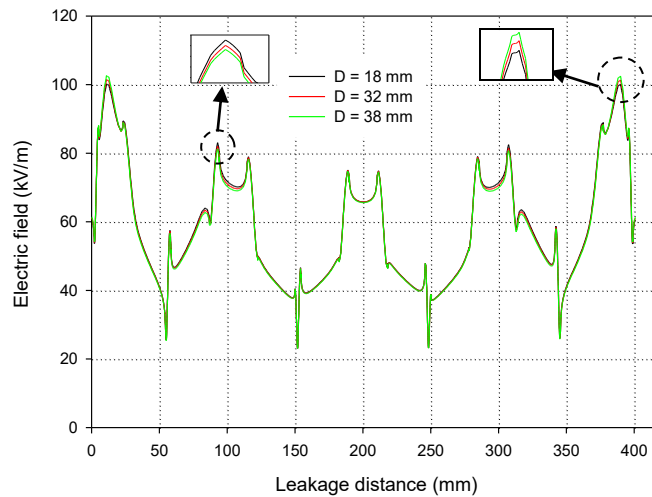


Figure 5: Electric field with different core diameter.

2.3. Effect of change of the shed’s radius:

In this case, the shed’s radius on the insulator was varied to simulate and study its effect in the electric field, as shown in Figure 6. The parameter is varied with values of 45 mm, 55 mm, and 65 mm to observe the effects of the electric field stress.

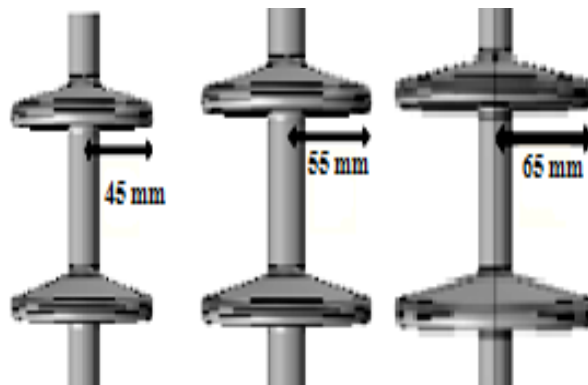


Figure 6: Change of the shed’s radius.

The electric field stress along the surface of the insulator is shown in Figure 7. From this figure, it is comprehended that the largest shed’s diameter generally yields the highest electric field stress [20]. However, at first shed’s outer corner, the electric field stress decreases as the shed’s radius increases.

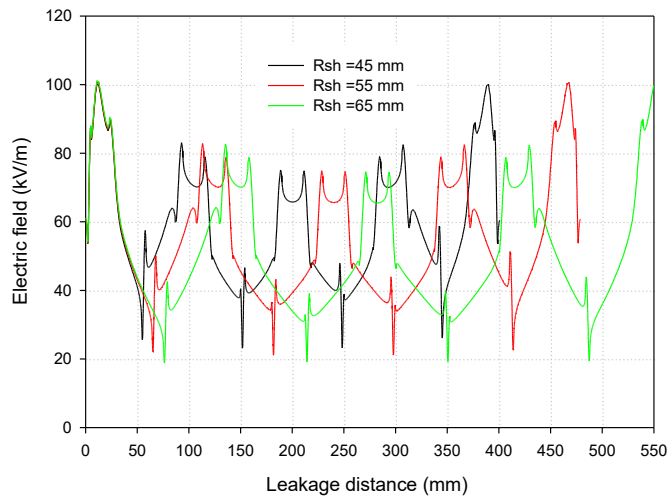


Figure 7: Electric field with different shed's radius.

2.4. Effect of change of the shed's inclination radius:

The shed's inclination radius of the 11kV SIR insulator is varied with values of 5 mm, 8 mm, and 12 mm as shown in Figure 8. The electric field stress along the surface of the insulator is shown in Figure 9. A slight change in the electric field in the surround of ground electrode region of the dielectric, while in the surround of high voltage area the field intensity increases with the increase of the shed's inclination radius as demonstrated in Figure 9.

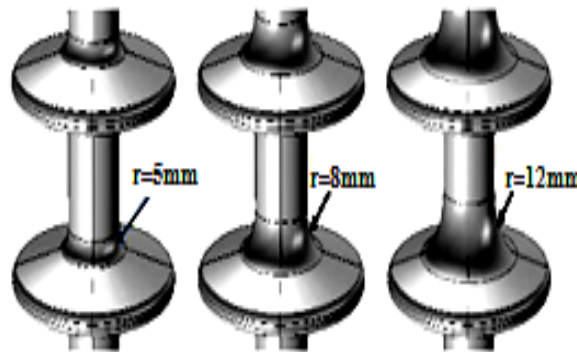


Figure 8: Change of the Shed's inclination radius.

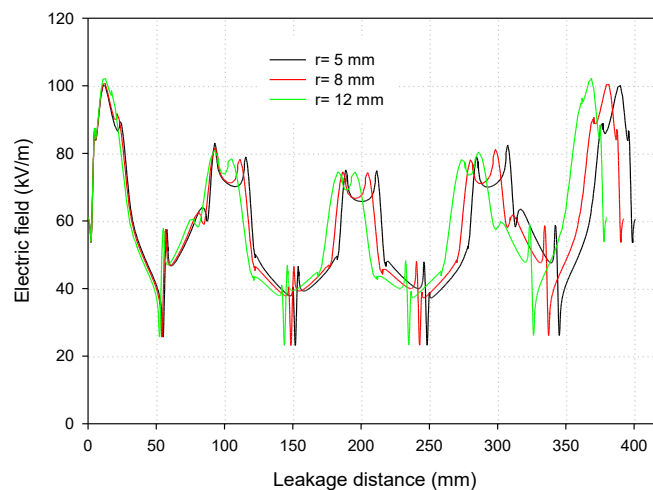


Figure 9: Electric field with different shed's inclination radius.

ARTIFICIAL NEURAL NETWORKS MODEL

Artificial neural network algorithms have been used successfully in many applications called "universal approximator", because of their ability to approximate any function, linear or no-linear, simple or complex. It transforms inputs into outputs to the best of its ability. An artificial neural network consists of a set of processing elements called neurons that interact by sending signals to one another along weighted connections (weights) [21]. Each neuron can have multiple inputs and outputs. Inputs to a neuron can be from external stimuli or can be from output of the other neurons. Copies of the single output that comes from a neuron can be input to many other neurons in the network. It is also possible that one of the copies of the neuron's output can be input to itself as feedback. An ANN can have three types of layers: the input layer, one or more hidden layers, and the output layer. When creating an ANN, it must first be decided how many neurons there will be in each layer. Therefore, a learning procedure is necessary in which the strengths of the connections are modified to achieve the desired form of activation function. The learning procedure is divided into three types: supervised, reinforced, and unsupervised. The type of error signal used to train the weights in the network defines these three types of learning. In supervised learning, an error scale is provided for each output neuron by an external "teacher", while in reinforced learning the network is given only a global punish/reward signal. In unsupervised learning, no external error signal is provided, but instead internal errors are generated between the neurons, which are then used to modify weights [22]. In a successful learning process, the weights are gradually modified in order to give an output close to the expected. An ANN is usually trained with the error back-propagation algorithm, in which the occurring errors of the output layer return in the input layer to modify the weights iteratively according to equation (5).

$$w_{ji}(n+1) = w_{ji}(n) + \Delta w_{ji}(n) \quad (5)$$

Where: $w_{ji}(n)$ and $w_{ji}(n+1)$ are the previous and the modified weights connected between the i^{th} and the j^{th} adjoining layers. $\Delta w_{ji}(n)$ stands for the correction or modification factor and n stands for the number of the iteration.

If we consider the j^{th} neuron in a single layer neural network, the training efficiency is enhanced by minimizing the error between the actual output of the j^{th} neuron and the output that has been dictated by the teacher. Same criterion can also be achieved by the use of a Least Squares Method (LSM). Hence, if there are L neurons in a particular network, the cost function to be ultimately minimized is given by equation (6).

$$e(n) = \frac{1}{2} \sum_{j=1}^L [d_j(n) - y_j(n)]^2 \quad (6)$$

Where $y_j(n)$ and $d_j(n)$ are respectively the actual and the teacher-requested outputs for the j^{th} neuron in the n^{th} iteration. The overall measure of the error for all the input-output patterns is given by

$$E(n) = \frac{1}{2} \sum_{n=1}^N \sum_{j=1}^L [d_j(n) - y_j(n)]^2 \quad (7)$$

Where N is the number of input-output patterns in the training set.

An ANN can have three types of layers: the input layer, one or more hidden layers, and the output layer. When creating an ANN it must first be decided how many neurons there will be in each layer. Therefore, a learning procedure is necessary in which the strengths of the connections are modified to achieve the desired form of activation function.

In this study, a neuronal model has been developed to estimate accurately the maximal electric field E_{max} . This model uses as input parameters the geometric characteristics of the insulators: shed radius R-sh, shed's inclination angle radius r, diameter of core D, and distance from the shed to the end fitting H, while the output variable is the maximal electric field E_{max} (Figure 10).

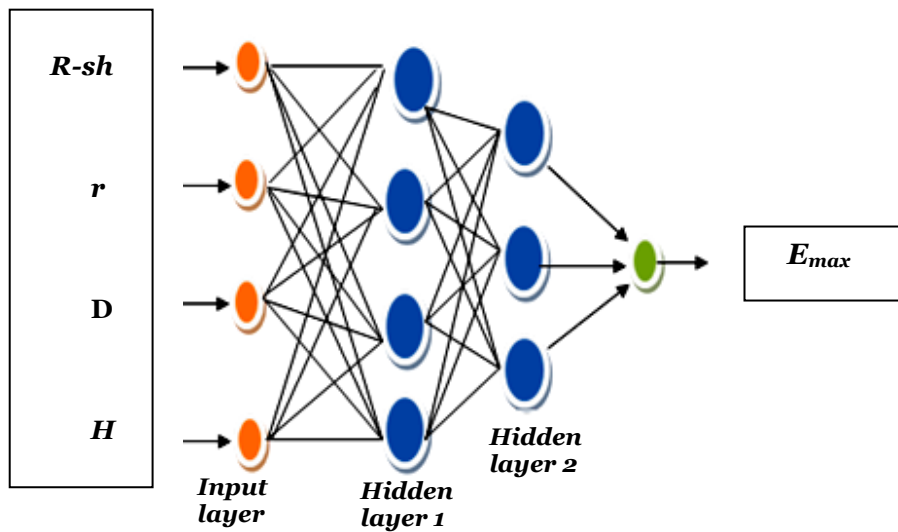


Figure 10: Structure of a Neuron Network multilayer.

In this paper, the prediction performances of the model are tested using the following statistical error criteria: the root mean square error (RMSE), the mean absolute percentage error (MAPE), and the absolute fraction of variance (R^2). These errors have been calculated by the following equations [23]:

$$RMSE = \sqrt{\frac{1}{N} \sum_{k=1}^N (d_k - y_k)^2} \quad (8)$$

$$R^2 = 1 - \sum_{k=1}^N \left(\frac{d_k - y_k}{d_k} \right)^2 \quad (9)$$

$$MAPE = \frac{1}{N} \sum_{k=1}^N \left[\left| \frac{d_k - y_k}{d_k} \right| \right] \cdot 100 \quad (10)$$

1. Normalization of the input/output data:

In order to avoid saturation phenomena and for better convergence of the learning process of the ANN model, the input and output variable values are normalized. The normalization is chosen by the maximum and minimum values of each variable, as shown in the following expression:

$$x_{i,nor} = a + \frac{b-a}{x_{max} - x_{min}} (x_i - x_{min}) \quad (11)$$

Where: $x_{min} = \min(x_i)$, $x_{max} = \max(x_i)$, a and b are the respective values of the normalized variable.

All the input-output variables in the training patterns are normalized within their series before the initiation of the training and test of the neural network.

2. Results and discussion:

In the present work, an ANN model was implemented by using the MATLAB software. The total number of vectors, which include the input and output variables, was 36. The 80% of these input-output patterns were decided to be used to train the network, while the rest 20% was used to test the function of the network. That means that the training set consisted of 29 vectors and the testing set consisted of 7 vectors. The training process was repeated until a root mean square error between the actual output and the desired output reaches the goal of 1.0% or a maximum number of epochs (it was set to 1500) are accomplished. The next step was to define the number of hidden layers, the number of neurons in each layer, the training method, the transfer function, and the number of epochs. Architecture and training

parameters of ANN were presented in Table 3.

Table 3: Architecture and training parameters.

Architecture	
The number of layers:	4
The number of neuron on the layers:	4/20/1
The initial weights and biases:	Random
Activation functions:	Logarithmic sigmoid
Training parameters	
Learning rule:	Levenberg–Marquardt Back-propagation
Learning rate :	0.25
Momentum constant:	0.85
Mean-squared error:	1E-10

Figure 11 presents the produced results of the ANN model for the training phase.

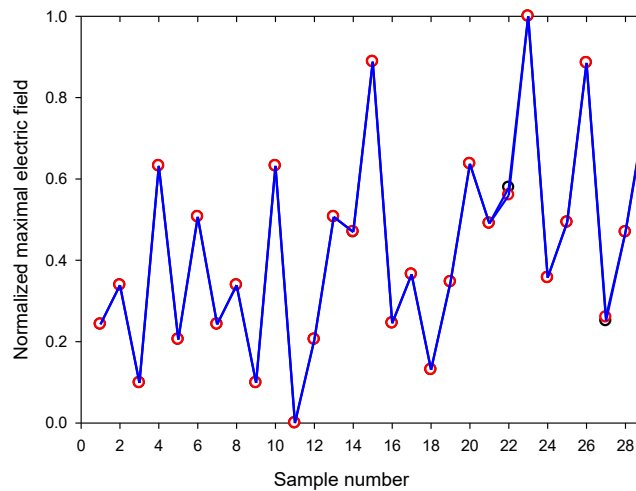


Figure 11: Training process of the ANN.

In order to validate the capability of the neural network model, its output is compared with the testing set (Figure 12).

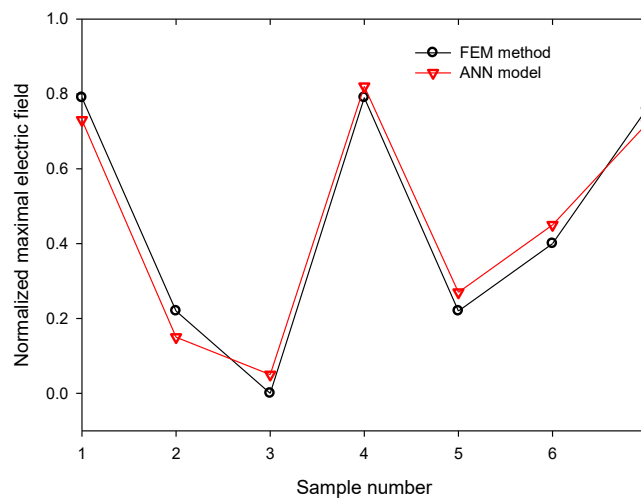


Figure 12: The comparison of the results of the ANN model and FEM results for Test.

The correlation between calculated and estimated targets for these cases is shown in figure 13. The results of the

comparison show that the ANN results and test results are nearly the same.

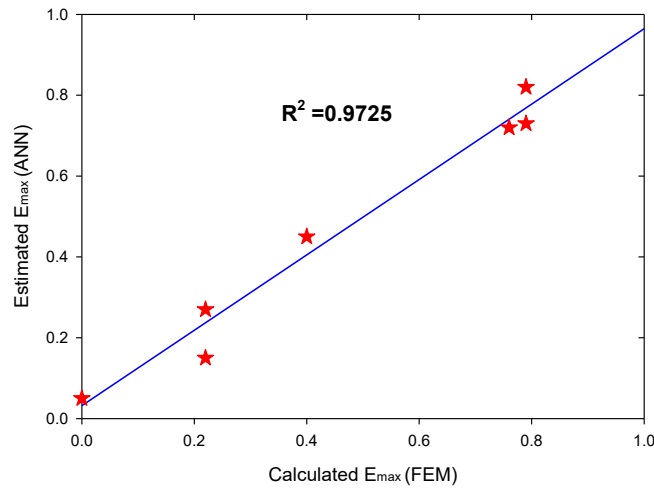


Figure 13: Correlation between estimated and calculated E_{max} .

The performance of the ANN model was measured by evaluation of the root mean square error (RMSE), the mean absolute percentage error (MAPE), and the correlation (R^2) between the predicted data and tested results.

Table 4 shows the values of the RMSE, MAPE, and (R^2) for both training and testing sets.

Table 4: Performance comparison in terms of the error statistics of the ANN model.

	RMSE	R^2	MAPE (%)
Training	0.0041	0.9997	0.28
Test- set	0.0052	0.9725	27.67

CONCLUSION

In this paper, the electric field on the surface of a composite suspension insulator under clean conditions has been estimated using an artificial neural network. The design variables of the insulators have been varied and analyzed, including shed radius, inclination angle radius, core diameter, and distance between the first shed and end fitting. First, it was used the Finite Element Method to evaluate the influence of insulator geometrical parameters on the electric field strength. Then, the ANN model was used to optimize the original profile that produces the lowest electric field strength. The principal characteristic of the proposed model is to set the optimum training parameters such as the number of neurons, learning rate, and momentum term. Our results reveal an acceptable degree of accuracy and low computation time. Therefore, this model can be used efficiently for the design and development processes of insulators. Future works are to be considered as a 3D study, using other recent algorithms and taking into account other constraints like wet and contamination conditions.

REFERENCES

- [1] El-Hag AH, Leakage current characterization for estimating the conditions of non-ceramic insulators surfaces, *Electr Power Syst Res* 2017; 77:379–84.
- [2] J. S. T. Looms, *Insulators for high voltages*, Peter Peregrinus Ltd, London, 1988.
- [3] Pouya Salehi, Amir Khorsandi, Behrooz Vahidi, Optimal design configuration of grading ring for polymeric insulator under different environmental conditions, *Electric Power Systems Research* 239 (2025) 111189 ISSN 0378-7796.
- [4] Liang, X.; Li, S.; Gao, Y.; Su, Z.; Zhou, J. Improving the outdoor insulation performance of Chinese EHV and UHV AC and DC overhead transmission lines. *IEEE Electr. Insul. Mag.* 2020, 36, 7–25.
- [5] Zhang, Z.; Pang, G.; Lu, M.; Gao, C.; Jiang, X. Study on decay-like fracture of 500 kV composite insulators: Infrared,

- ultraviolet and electric field distribution detection. *IET Gener. Transm. Distrib.* 022, 16, 4132–4141.
- [6] Song Gao, Yunpeng Liu, Le Li. A Comparative Study of Abnormal Heating Composite Insulators. *Polymers* 2023, 15, 2772. <https://doi.org/10.3390/polym15132772>.
- [7] A. Tzimas, C. Zachariades, and S. Rowland, "Electric field analysis of 132kv epdm insulator and correlation with ageing features", in *Electrical Insulation Conference (EIC)*, 2013 IEEE, pp. 210–214, IEEE, 2013.
- [8] R. A. Rifai, A. H. Mansour, and M. A. H. Ahmed, "Estimation of the electric field and potential distribution on three dimension model of polymeric insulator using finite element method," 2015, *IJEDR | Volume 3, Issue 2 | ISSN: 2321-9939*, pp. 694–705.
- [9] Arshad, Nekahi, A., McMeekin, S. G., & Farzaneh, M. "Numerical computation of electric field and potential a long silicone rubber insulators under contaminated and dry band conditions", *3D Research*, 7(25). 10.1007/s13319-016-0101-z, (2016).
- [10] M.V.K. Chari, G. Bedrosian, J. d'Angelo, A. Konrad, *Finite element applications in electrical engineering*, IEEE Trans. Magn. 29 (2) (1993) 1306–1314.
- [11] B. Zhang, S. Han, J. He, R. Zeng, P. Zhu, Numerical analysis of electric-field distribution around composite insulator and head of transmission tower, *IEEE Trans. Power Deliv.* 21 (2) (2006) 959–965.
- [12] E.T. Moyer, E.A. Schroeder, Finite element formulations of Maxwell's equations advantages and comparisons between available approaches, *IEEE Trans. Magn.* 27(5) (1991) 4217–4220.
- [13] P.S. Ghosh, S. Chakravorti, N. Chatterjee, "Estimation of time-to-flashover characteristics of contaminated electrolytic surfaces using a neural network", *IEEE Trans. Dielectr. Electrical Insulation* 2 (6) (1995) 1064–1074.
- [14] M. Marich, H. Hadi, Evaluation of flashover voltage on polluted insulators with artificial neural network, *JEE*, Volume N°03, pp 248-253, September 2015.
- [15] M. Ugur, D.W. Auckland, B.R. Varlow, Z. Emin, Neural networks to analyze surface tracking on solid insulators, *IEEE Trans. Dielectr. Electrical Insulation* 4 (6) (1997) 763–766.
- [16] A.S. Ahmad, P.S. Ghosh, S. Shahnawaz Ahmed, S.A.K. Aljunid, Assessment of ESDD on high-voltage insulators using artificial neural network, *Elsevier Electr. Power Syst. Res.* 72 (2) (2004) 131–136.
- [17] V. T. Kontargyri, A. A. Gialketsi, G.J. Tsekouras, I.F. Gonos, I.A. Stathopoulos, Design of an artificial neural network for the estimation of the flashover voltage on insulators, *Electric Power Systems Research*, Vol. 77, pp.1532–1540, 2007
- [18] Sajjad, U., Arshad, A., Ahmad, J., & Shoaib, S. Application of artificial neural network in predicting flashover behaviour of outdoor insulators under polluted conditions. In *2021 IEEE Conference of Russian Young Researchers in Electrical and Electronic Engineering (ElConRus)* (2021) (pp. 2868-2873). IEEE.
- [19] Ali. A. Salem, R. Abd-Rahman, M. S. Kamarudin, H. Ahmed, N.A.M. Jamail, N.A. Othman, M.F.M. Yousof, M. T. Ishak, S. Al-Ameri "The effect of insulator geometrical profile on electric field distributions", *Indonesian Journal of Electrical Engineering and Computer Science*, Vol. 14, No. 2, May 2019, pp. 618-627, ISSN: 2502-4752.
- [20] B. Marungsri, W. Onchantuek, A. Oonsivilai and T.Kulworawanichpong "Analysis of electric Field and Potential Distributions along Surface of Silicone Rubber Insulators under contamination Conditions Using Finite Element Method" *World Academy of Science, Engineering and Technology* 53, pp. 1353- 1363, 2009.
- [21] S. Haykin, *Neural Networks: a Comprehensive Foundation*, Upper Saddle River, N.J., Prentice Hall, 1999.
- [22] S. H. Ngia, Efficient training of neural nets for nonlinear adaptive filtering using a recursive Levenberg-Marquardt algorithm, *IEEE Trans. On Signal Processing*, Vol. 48, pp. 1915-1927, 2000.
- [23] Gencoglu, M.T., Uyar, M., (2009). Prediction of flashover voltage of insulators using least square support vector Machines, *Expert Syst. Appl.* 36,10789–10798.